
STUDYING THE RESPONSE OF THE MID-LATITUDE IONOSPHERE OF THE NORTHERN HEMISPHERE TO MAGNETIC STORMS IN MARCH 2012

M.A. Chernigovskaya 

*Institute of Solar-Terrestrial Physics SB RAS,
Irkutsk, Russia, cher@iszf.irk.ru*

†B.G. Shpynev

*Institute of Solar-Terrestrial Physics SB RAS,
Irkutsk, Russia*

D.S. Khabituev

*Institute of Solar-Terrestrial Physics SB RAS,
Irkutsk, Russia, Khabituev@iszf.irk.ru*

K.G. Ratovsky

*Institute of Solar-Terrestrial Physics SB RAS,
Irkutsk, Russia, ratovsky@iszf.irk.ru*

A.Yu. Belinskaya 

*Trofimuk Institute of Petroleum Geology and Geophysics SB RAS,
Novosibirsk, Russia, BelinskayaAY@ipgg.sbras.ru*

A.E. Stepanov

*Yu.G. Shafer Institute of Cosmophysical Research
and Aeronomy SB RAS,
Yakutsk, Russia, a_e_stepanov@ikfia.sbras.ru*

V.V. Bychkov

*Institute of Cosmophysical Researches and Radio Wave Propagation
of the FEB RAS,
Paratunka, Russia, vasily.v.bychkov@gmail.com*

S.A. Grigorieva

*Institute of Geophysics UB RAS,
Ekaterinburg, Russia, ion@arudaemon.gsras.ru*

V.A. Panchenko

*Pushkov Institute of Terrestrial Magnetism, Ionosphere
and Radiowave Propagation, RAS,
Moscow, Troitsk, Russia, panch@izmiran.ru*

J. Mielich

*Leibniz Institute of Atmospheric Physics,
Kühlungsborn, Germany, mielich@iap-kborn.de*

Abstract. We have studied variations in ionospheric and geomagnetic parameters in the Northern Hemisphere during a series of magnetic storms in March 2012 by analyzing data from the Eurasian mid-latitude ionosonde chain, mid- and high-latitude chains of magnetometers of the global network INTERMAGNET. We have confirmed manifestations of the longitude inhomogeneity of ionospheric effects, which is associated with the irregular structure of the longitudinal variability of geomagnetic field components. The complex physics of the long magnetically disturbed period in March 2012 with switching between positive and negative phases of the ionospheric storm in the same period of the magnetic storm for different spatial

regions is emphasized. The change in the effects of the ionospheric storm during this period might have been associated with the superposition in the mid-latitude region of the competing processes affecting the ionospheric ionization whose sources were in the auroral and equatorial ionosphere. We have compared the scenarios for the development of ionospheric disturbances under equinox conditions during magnetic storms in March 2012, October 2016, and March 2015.

Keywords: ionosonde chain, ionospheric disturbances, geomagnetic field variations, geomagnetic storm.

INTRODUCTION

The cause of disturbances in Earth's ionosphere is often a sequence of interrelated events that begin with processes of increased solar activity (solar flares, coronal mass ejections, high-speed streams from coronal holes), which then affect the solar wind — magnetosphere — ionosphere system. In other cases, ionospheric disturbances are caused by internal factors of the ionosphere and thermosphere, which are related to processes in the underlying neutral atmosphere. In both cases, ionospheric ionization disturbances of different intensity and different spatial and temporal scales occur.

Under increased solar activity, the solar wind velocity increases sharply. The effective exchange of solar wind energy with near-Earth space leads to serious changes in

currents, fields, and plasma of the magnetosphere, thereby causing significant disturbances in the geomagnetic field (GMF) strength — a geomagnetic storm, which is a vivid manifestation of heliogeomagnetic activity [Dudok de Wit, Watermann, 2009]. Effective conditions for the transfer of solar wind energy to Earth's magnetosphere are long (from a few to many hours) periods of high-speed solar wind and, what is most important, the interplanetary magnetic field (IMF) B_z component southward and opposite to the GMF direction in the dayside magnetosphere. There is reconnection (merging) between IMF lines with the southward B_z component and the GMF lines open in the polar regions. At the same time, a strong dawn-to-dusk electric field is induced in the polar cap, which can lead to abrupt changes in Earth's ionosphere. The perturbed electric fields have been identified by Tsurutani et al. [2004] as (1) almost

instantly appearing zonal prompt penetration electric fields (PPEFs), often observed in equatorial latitudes; (2) electric fields with a delay created by a perturbed dynamo as a result of Joule heating due to energy input during a magnetic storm at high latitudes, which can cause large rises or downward flows of ionospheric plasma leading to large-scale increases or decreases in ionization and vertical total electron content (TEC).

In response to intensive energy release in the magnetosphere and polar ionosphere during magnetic storms, chemical and dynamic/electrodynamic processes in the global ionosphere—thermosphere system change significantly. Ionospheric plasma densities, the gas composition of the neutral thermosphere, and the dynamics of the mid-latitude, low-latitude, and equatorial atmosphere and ionosphere are redistributed [Blanc, Richmond, 1980].

The ionospheric response to the magnetosphere-ionosphere coupling during a magnetic storm is known as an ionospheric storm [Hafstad, Tuve, 1929; Prölss, 1995; Prölss et al., 1991; Buonsanto, 1999]. Ionospheric storms are accompanied by significant variations in the F2-layer critical frequency f_oF2 , which is proportional to the F-region peak electron density [Polyakov et al., 1968]. Under disturbed conditions, f_oF2 may increase, but its sharp decrease is more often observed as compared to the values under quiet conditions (positive or negative ionospheric storms respectively) [Matsushita, 1959]. The occurrence of positive and negative effects of ionospheric storms strongly depends on the local time, season, and geographic region [Prölss, 1995; Rishbeth, 1998; Buonsanto, 1999; Mendillo, 2006; Burešová et al., 2007]. Negative ionospheric storms are the dominant characteristic in the ionospheric response to increased geomagnetic activity and are generally attributed to changes in the neutral composition and to the shift of the main ionospheric trough toward the equator [Prölss, 1995; Rishbeth, 1998].

Positive ionospheric storms are caused by an increase in equatorward neutral winds occurring due to energy inflow to auroral latitudes during a magnetic storm [Prölss, 1995]. During positive ionospheric storms, the effects of neutral winds prevail over changes in the chemical composition at midlatitudes.

Another reason for the effects of a positive ionospheric storm is the processes in the equatorial latitudes during geomagnetic storms. In the equator, the electrodynamic drift enhanced by PPEFs $\vec{E} \times \vec{B}$ causes ionospheric plasma to move upward to 800–1000 km [Astafyeva, 2009]. Plasma transfer from the near-equator region to higher altitudes and higher latitudes forms a giant plasma fountain (dayside ionospheric super fountain) [Tsurutani et al., 2004]. According to [Danilov, 2013], PPEFs are responsible for the positive phases of ionospheric storms observed at low and middle latitudes even during moderate storms. These fields mask the effects of negative ionospheric storms. Photoionization of the lower F-region produces a “new” plasma that compensates for that uplifted under the influence of the drift $\vec{E} \times \vec{B}$, which leads to an increase in TEC — the dominant effect in midlatitudes.

Most studies into the spatial dependencies of ionospheric responses to geomagnetic activity are limited to a specific latitude-longitude region, although there are studies into the global distribution of electron density [Mansilla, 2004; Astafyeva et al., 2015; Kunitsyn et al., 2016]. Many of these studies have been carried out using satellite measurements of atmospheric and ionospheric parameters. There has been tremendous progress in developing these measurements recently. But there are also studies based on experimental data from networks of ground-based radio-physical stations or complex studies combining ground and satellite measurements. To examine the spatio-temporal variations in ionospheric parameters by ground-based methods, experimental measurements made at meridional instrument chains are more often employed. In such cases, latitudinal distributions of ionospheric parameters are analyzed. Latitude variations in ionization manifest themselves most clearly and vividly, their explanation is more obvious, especially in the case of analyzing the influence of heliogeomagnetic disturbances on the ionosphere. Longitude variations in the distributions of ionospheric parameters under quiet and especially disturbed geomagnetic conditions are analyzed much less frequently [Mansilla, 2004; Dmitriev et al., 2013; Wang, Zhang, 2017; Li et al., 2018; Mansilla, Zossi, 2020]. Such studies are therefore highly relevant. Of particular importance is to examine the physical mechanisms responsible for the formation of longitudinal effects in the ionosphere.

At the previous stage of research based on data from the Eurasian mid-latitude ionosonde chain, as well as mid- and high-latitude chains of GPS/GLONASS receivers and INTERMAGNET magnetometers, the longitude features of the ionospheric response to extreme magnetic storms in March and June 2015 [Shpynev et al., 2018; Chernigovskaya et al., 2019, 2020 2021a] and to the strong magnetic storm in October 2016 [Chernigovskaya et al., 2021b] were addressed for the first time. The main cause of the detected longitude variations in ionospheric parameters was the configuration of the main geomagnetic field, as well as the mismatch of the magnetic and geographic poles (known as UT variations). In this paper, we continue to analyze the ionospheric effects of magnetic storms, using the proven method of analyzing geomagnetic and ionospheric data for the series of magnetic storms in March 2012.

EXPERIMENTAL MEASUREMENT DATA

In this paper, to analyze the response of the ionosphere to a geomagnetic storm, we employ the following data on: 1) hourly average values of the critical frequency f_oF2 and the height of the ionization maximum h_mF2 of the ionospheric F2 layer from measurements made at a chain of seven mid-latitude ionosondes (Figure 1 and Table); 2) the H and Z components of the GMF strength with one-minute resolution from measurements made at mid- and high-latitude chains of magnetometers of the global network INTERMAGNET [<http://www.intermagnet.org>] (Figure 1).



Figure 1. Layout of the ionosonde chain (white circles) and magnetometer chains (red and blue marks)

The Eurasian chain (white circles in Figure 1; Table) includes the ionosonde AIS (Paratunka), two Russian ionosondes Parus of various modifications (Novosibirsk, Ekaterinburg), and four digital ionosondes DPS-4 of various modifications (Yakutsk, Irkutsk, Moscow,

Juliusruh). The time resolution for different ionosondes varies from 15 min to 1 hr (for Parus ionosondes). Older models of ionosondes operate with less transmitter power; therefore, they have interruptions during the main phase of strong storms. The gaps in the time series of ionosonde measurements were replaced by linear interpolation of adjacent available measurements.

We analyzed hourly average values of f_oF2 and h_mF2 as well as variations in absolute deviations df_oF2 and dh_mF2 of these parameters from the background level. This is especially important when analyzing h_mF2 variations to eliminate the ambiguity in identifying this parameter at ionosondes of different types. Background values were calculated by averaging $f_oF2(t)$ and $h_mF2(t)$ by a running mean over a smoothing interval of $(t-14, t+14)$ days before and after each hour t of the current day. Then, using the time series of hourly initial data on $f_oF2(t)$ and $h_mF2(t)$, we calculated the series of absolute deviations $df_oF2(t)$ and $dh_mF2(t)$ from the background level.

During the magnetic disturbances of interest, there were short data gaps at the ionosonde Parus-3.0 in Ekaterinburg. There is also no AIS ionosonde data in Paratunka for March 19, 2012.

Stations of the mid-latitude ionosonde chain

Station	Ionosonde type	Geographic coordinates		Geomagnetic coordinates	
		Latitude	Longitude	Latitude	Longitude
Juliusruh	DPS-4D	55° N	13° E	54° N	99° E
Moscow	DPS-4	56° N	37° E	52° N	122° E
Ekaterinburg	Parus 3.0	57° N	60° E	50° N	141° E
Novosibirsk	Parus 1.0	55° N	83° E	50° N	160° E
Irkutsk	DPS-4	52° N	104° E	42° N	177° E
Yakutsk	DPS-4	62° N	130° E	53° N	163° W
Paratunka	AIS	53° N	158° E	46° N	138° W

ANALYZING HELIOGEOMAGNETIC CONDITIONS AND GMF VARIATIONS

The period of increased geomagnetic activity we analyze consists of a series of four magnetic storms: March 7, 9, 12 and 15, 2012. (S1–S4 events respectively in Figure 2). Solar activity was high during March 5–7, 9, 10, 13, and 14 largely due to a series of long large solar flares X1.1 on March 5, X5.4 on March 7, M6.3 on March 9, M8.4 on March 10, M7.9 on March 13, and M2.8 on March 14 from active region 1429 [Tsurutani et al., 2014]. All the flares were linked to earthward coronal mass ejections (CMEs). During the period from March 16 to March 18 under study (the S4 magnetic storm), there was a coronal hole high-speed stream (CH HSS). It is well known that CH HSS events cause an increase in geomagnetic activity. All the four magnetic storms are associated with an increase in the solar wind

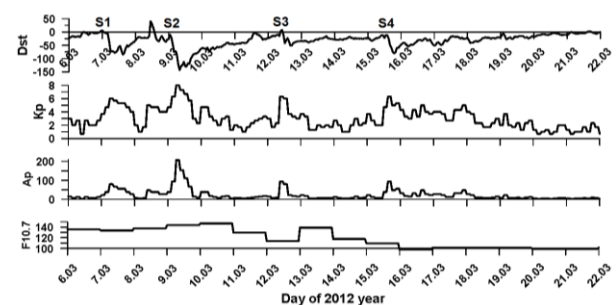


Figure 2. Time variations in the heliogeomagnetic activity indices Dst , K_p , A_p , $F10.7$ during a series of magnetic storms in March 2012

velocity, plasma density and temperature, as well as in the IMF strength. The high solar wind velocities are driven by earthward CMEs and CH HSS.

The magnetic storm S1 began on March 7 after the arrival of the CME associated with the X1.1 flare of March 5. At the maximum of the storm on March 7,

2012 at 15:00 UT, Dst decreased to -85 nT, K_p increased to 6_o , A_p was as high as 80 nT [<http://wdc.kugi.kyoto-u.ac.jp>] (see Figure 2). The March 7–8, 2012 magnetic storm was moderate according to the Dst classification [Loewe, Prölss, 1997]; it belongs to class G2 (moderate) according to the NASA classification [<https://www.swpc.noaa.gov/noaa-scales-explanation>].

The most intense was the magnetic storm S2 on March 9–11, 2012. It is associated with the X5.4 flare on March 7 (the most powerful during the period of interest) and with the accompanying CME that reached Earth about two days later, according to NOAA SWPC (Space Weather Prediction Center) PRF 1906 (Preliminary Report and Forecast) of March 13, 2012. Geomagnetic activity increased from the level of a weak storm on March 8 to a strong one on March 9 (class G4) due to steady southward IMF B_z in combination with the continuing effect of CME. Activity decreased to the level of a weak storm by March 10 with gradually decreasing CME effects. Return to quiet geomagnetic conditions took place on March 11. At the maximum of the storm on March 9, 2012 at 08:00 UT, Dst decreased to -143 nT, K_p increased to 8_o ; A_p was as high as 207 nT [<http://wdc.kugi.kyoto-u.ac.jp>] (see Figure 2).

The third magnetic storm S3 began on March 12 as a result of the March 9 M6.3, March 10 M8.4 solar flares, and the accompanying CMEs. At the maximum of the storm on March 12, 2012 at 16:00 UT, Dst decreased to -51 nT, K_p increased to 6_+ , A_p was as high as 94 nT [<http://wdc.kugi.kyoto-u.ac.jp>] (see Figure 2). Return to quiet geomagnetic conditions occurred on March 13, 14. The March 12–14, 2012 magnetic storm was moderate (class G2).

The fourth magnetic storm S4 began on March 15 after the arrival of CMEs driven by the March 13 M7.9 and March 14 M2.8 solar flares. At the maximum of the storm on March 15, 2012 at 19:00 UT, Dst decreased to -80 nT, K_p increased to 6_+ ; A_p run to 94 nT [<http://wdc.kugi.kyoto-u.ac.jp>] (see Figure 2). The storm was accompanied by a CH HSS event that lasted from March 16 to March 18 after the S4 magnetic storm main phase, which caused the storm recovery phase to extend. It is known that CH HSS events usually have a weak effect on Dst , but are reflected in A_p and K_p variations (see Figure 2). The March 15–19, 2012 magnetic storm was moderate (class G2).

The solar activity index $F10.7$ during the period considered varied from 147 to 100 (in 10^{-22} W/($m^2 \cdot Hz$)) (see Figure 2, bottom panel).

As the main parameter when analyzing the GMF variability, we utilize the variance of the GMF strength H and Z components (standard deviation relative to background undisturbed values). Using data from two chains of INTERMAGNET magnetometers at middle and high latitudes (see Figure 1), we have obtained longitudinal distributions of the GMF strength H - and Z -component variances for the periods of the March 2012 magnetic storms under study, as well as on quiet days before the onset of geomagnetic disturbances (Figure 3).

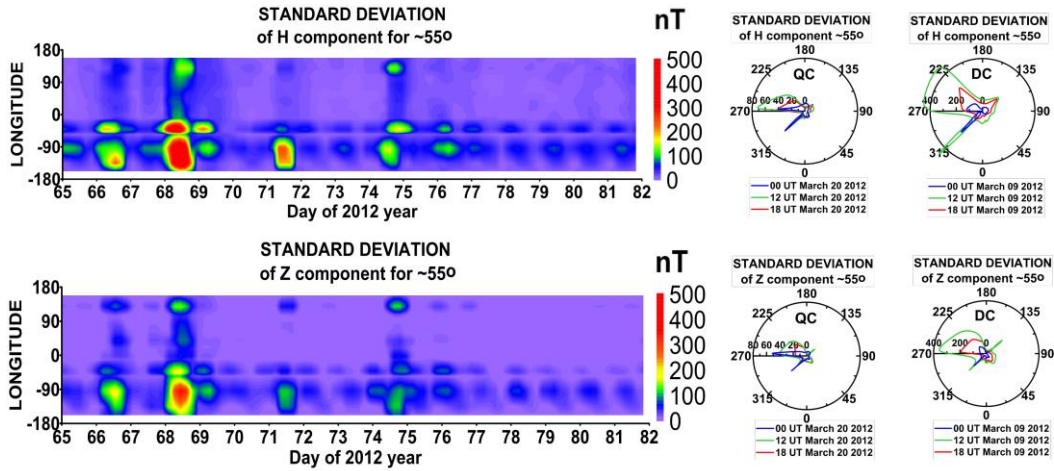
In the longitudinal distribution of GMF variations, as in our previous studies, we identified pronounced longitudes at which the intensity of the variations had maxima and minima. In most cases, the maximum irregularities of the longitude variations in the GMF variances are observed at midlatitudes (near $\sim 55^\circ$ N) (Figure 3, *a*). Note that for the magnetic storm period March 7–20, 2012 the maximum variations in the GMF components occurred in the Western Hemisphere in the direction of the geomagnetic pole meridian near $\sim 270^\circ$ ($\sim 90^\circ$ W in geographic coordinates) and at longitudes of $\sim 225^\circ$ ($\sim 135^\circ$ W) and $\sim 315^\circ$ ($\sim 45^\circ$ W). The zone of strong GMF variations at $\sim 120^\circ$ – 140° E longitudes was most pronounced in the Eastern Hemisphere during the magnetically disturbed period over Eurasia. At high latitudes (near $\sim 70^\circ$ N), the GMF variability is more uniform in longitude (Figure 3, *b*), but longitude inhomogeneities of the GMF variations also manifest themselves.

ANALYSIS OF MEASUREMENT DATA FROM THE MID-LATITUDE IONOSONDE CHAIN

Figure 4 shows the longitude-time variations in the ionization parameters of the F2 layer as detected by the chain of seven mid-latitude ionosondes. Vertical dashed lines indicate sudden storm commencements (SSC) in March 2012 caused by the impact of interplanetary shock waves on Earth's magnetosphere. During the equinox period considered, there is a pronounced day–night transition in f_oF2 variations. The slope of the daily maxima and minima of the ionization parameters corresponds to the difference in the local time of the receiving stations. The gray color indicates the period of absence of AIS measurement data in Paratunka on March 19, 2012.

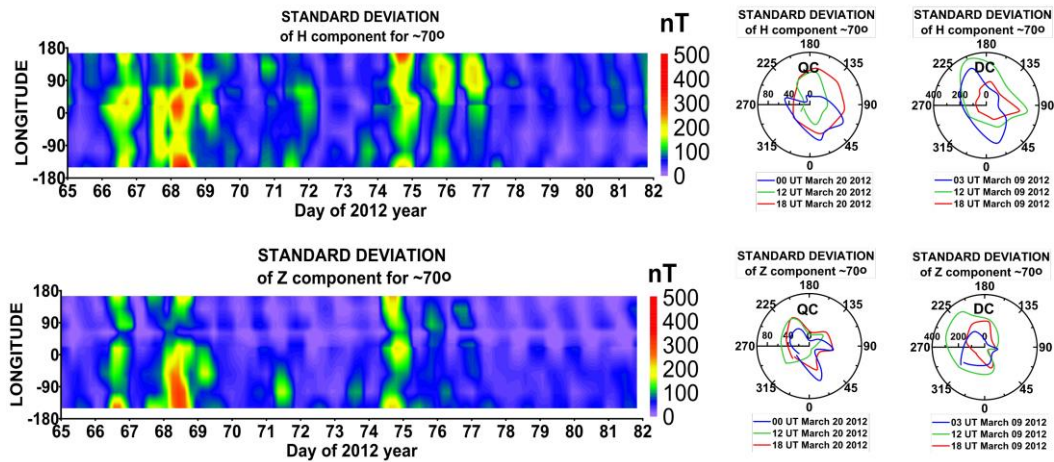
Immediately after SSC of the magnetic storm S1 on March 7, there was a significant increase in the F-region electron density according to the data from the Far Eastern ionosondes Paratunka, Yakutsk, (f_oF2 increased by 2–3 MHz) (panel *b*). The F2-layer critical frequencies reached values of ~ 9 MHz (panel *a*). The effect of a positive ionospheric storm over the Far East was observed during the magnetic storm main phase. During the recovery phase, the ionization response to the geomagnetic disturbance over Paratunka and Yakutsk was replaced by the effect of a negative ionospheric storm. A particularly strong decrease in the F-region electron density occurred on March 8 over Paratunka (f_oF2 decreased by 3–3.5 MHz) (panel *b*). The ionosphere did not recover to the quiet level. The next magnetic storm S2 was the most intense of the series of March 2012 storms. Geomagnetic activity increased from the level of a weak storm on March 8 to a strong one (class G4) on March 9 ($Dst = -143$ nT) (see Figure 2). The negative ionospheric storm effect was very pronounced in Paratunka and Yakutsk ionosonde data. The F2-layer critical frequency decreased to 1.9 MHz in Paratunka (panel *a*). The ionosphere over the mid-latitude region of the Far East after the strong storm on March 9 did not have time

Mid latitudes



a

High latitudes



b

Figure 3. Longitude-time variations in GMF H - and Z -component variances on March 6–22, 2012 and distributions of the GMF variances in polar coordinates for individual days of March 2012 for quiet conditions (QC, left column) and disturbed conditions (DC, right column) at middle $\sim 55^\circ$ N (a) and high $\sim 70^\circ$ N latitudes (b)

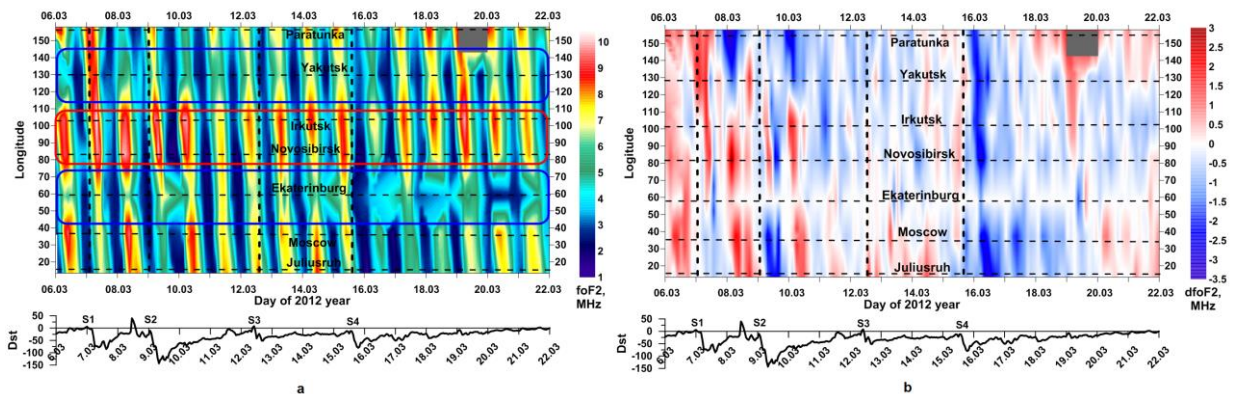


Figure 4. Longitude-time variations in f_oF_2 (a) and absolute deviations df_oF_2 (b) as detected by the mid-latitude ionosonde chain during a series of storms in March 2012. Vertical dashed lines show SSC of the storms; the bottom panel displays Dst variations

to recover until SSC of the next moderate magnetic storm S3 on March 12, which was the weakest in the series of the March 2012 magnetic storms under study ($Dst=-51$ nT) (see Figure 2). Thus, the significant decrease in ionization in the F2 layer (f_oF2 decreased by $\sim 2-3$ MHz) (panel *b*) was observed during the S1 storm recovery phase, the entire storm S2, and the entire storm S3 almost until March 14 when the ionosphere partially recovered to the quiet level.

Over Siberia, according to ionosondes in Irkutsk and Novosibirsk, the ionosphere during the storm S1 on March 7 exhibited the effect of a positive ionospheric storm (f_oF2 increased by $2-3$ MHz) (panel *b*) during both the magnetic storm main and recovery phases. A particularly significant increase in the F-region electron density was observed over Novosibirsk during the storm recovery phase on March 8, f_oF2 reached a value of 10.3 MHz (panel *a*). This might have been a manifestation of the after-effect of magnetic storms [Ratovsky et al., 2018], which consists in the formation of positive disturbances of the electron density in the daytime a few days after the onset of the recovery phase; in this case, the ionization values may exceed the level of quiet days before the beginning of a magnetic disturbance. Over Siberia, the ionospheric response to the March 9 strong magnetic storm S2 was also positive during the storm main phase (f_oF2 increased by $2.5-3$ MHz) (panel *b*). The F2-layer critical frequencies on March 9 were as high as 10.26 and 10.2 MHz in Irkutsk and Novosibirsk respectively (panel *a*). In the second half of March 9, there was a short-term change in the ionospheric response from positive to negative. But during the magnetic storm recovery phase on March 10, the ionization values again exceeded the background ones by $2-3$ MHz (panel *b*). The F2-layer critical frequency reached 10.4 MHz in Irkutsk (panel *a*).

By the end of March 10, the ionospheric response became negative again (f_oF2 decreased by $3-3.5$ MHz) (panel *b*). The negative ionospheric storm effect from that moment was similar to that observed for the Far East, as detected by the Paratunka and Yakutsk ionosondes. Ionization of the ionosphere over midlatitudes of Siberia and the Far East was reduced compared to quiet geomagnetic conditions. The ionosphere did not recover until SSC of the next moderate magnetic storm S3 on March 12. A significant decrease in ionization in the F2 layer (f_oF2 decreased by $\sim 2-3$ MHz) (panel *b*) was observed during the S3 magnetic storm main and recovery phases almost until March 14 when the ionosphere partially recovered to the quiet level.

Note that with a partial similarity between the scenarios for the development of ionospheric storms over the Far East and Siberia during the recovery phase of the strong magnetic storm on March 9 and during the entire moderate magnetic storm on March 12, the ionospheric ionization level over Siberia was higher than over the Far East (panel *a*).

Ionospheric ionization according to the Ekaterinburg ionosonde data was reduced during all the magnetic storms under study as compared to the neighboring regions of Siberia and Europe (panel *a*). How-

ever, it is worth repeating that there were failures in the operation of the ionosonde Parus-3.0 in Ekaterinburg and, as a result, moments of absence of measurements. We cannot therefore analyze the ionospheric response to magnetic storms in detail.

According to European ionosondes in Moscow and Juliusruh, during the magnetic storm S1 on March 7 there was a slight decrease in f_oF2 by $1-1.5$ MHz (panel *b*). For Europe, the negative ionospheric storm effect was observed until the ionosphere recovered to undisturbed conditions on March 8, 2012. With the onset of the strong magnetic storm S2 on March 9, 2012, the ionosphere over Europe revealed the properties of a negative ionospheric storm during the main and recovery phases until March 10, when the ionospheric response became positive for a short time. On March 11, the ionospheric ionization began to recover to the quiet level. The ionosphere responded to the moderate storm S3 on March 12 with a slight increase in ionization (f_oF2 increased by $1-2$ MHz) (panel *b*).

The response of the mid-latitude ionosphere over Eurasia to the moderate storm ($Dst=-80$ nT) that began on March 15 (S4) was very interesting (see Figure 2). During the recovery phase from March 16 to March 18, the storm was accompanied by a CH HSS event, which led to the extension of the storm recovery phase. According to the data from all mid-latitude ionosondes over the territory of Eurasia, the negative ionospheric storm effect was manifested during the main and recovery phases of the magnetic storm. The minimum values of ionization were observed over Western Europe. The F2-layer critical frequency was as high as 1.3 MHz on March 16, 2012, according to the Juliusruh ionosonde data (panel *a*). The negative ionospheric storm lasted until March 20 over a vast region of Eurasia, according to the data from ionosondes in Ekaterinburg, Moscow, and Juliusruh. Since March 20, ionization of the ionosphere began to recover to the quiet level. Over Siberia (ionosondes in Irkutsk and Novosibirsk) and the Far East (ionosonde in Paratunka), the ionosphere began to recover on March 18, 2012 — earlier than over Europe.

Figure 5 illustrates variations in absolute deviations dh_mF2 of the F2-layer maximum heights from the background level. During magnetic storms, the magnetospheric convection zone shifts from high to middle latitudes. GMF flux tubes with large L (L is the distance to the top of the geomagnetic field line in Earth radii) and low plasma concentration move to midlatitudes. Ionospheric plasma flows up rapidly, reducing the ionization density at the F2-layer maximum (thereby decreasing f_oF2) and increasing h_mF2 .

Significant increases in the ionization maximum (by more than 100 km) were recorded during negative ionospheric storms: for the moderate magnetic storm S1 — during the storm recovery phase on March 7 according to ionosondes in Irkutsk, Novosibirsk, Ekaterinburg, Moscow, Juliusruh and during the storm recovery phase on March 8 according to the ionosonde in Paratunka; for the strong magnetic storm S2 — during the storm main

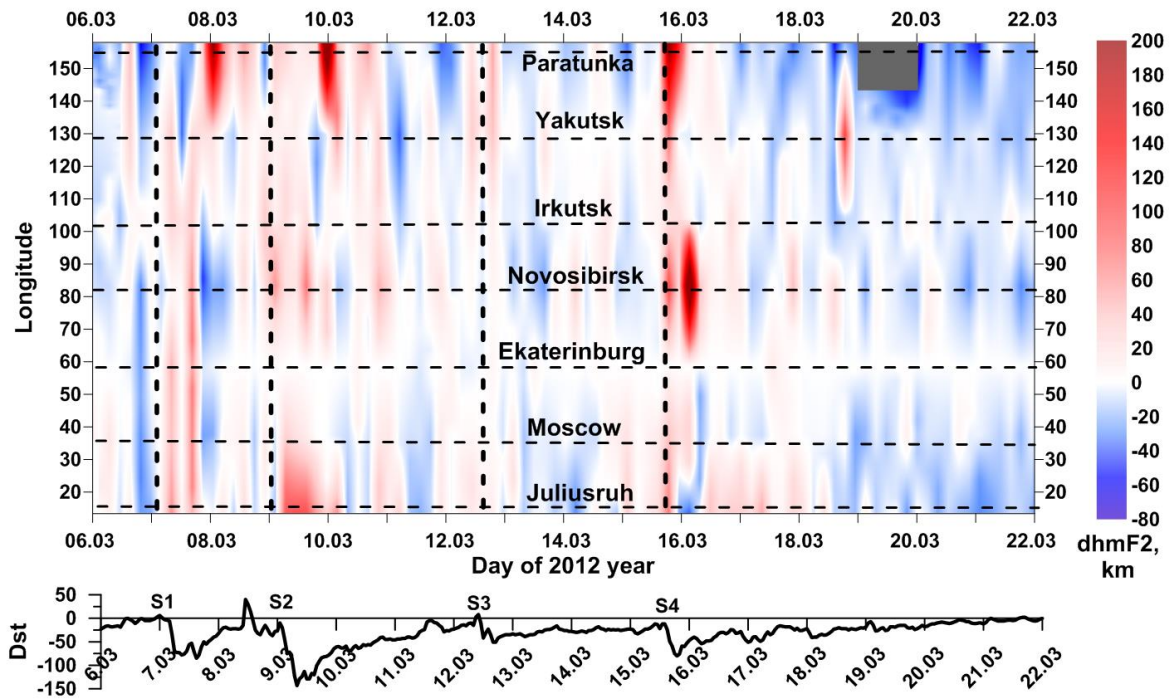


Figure 5. Longitude-time variations in absolute deviations of the maximum ionization height dh_mF2 according to the data from the mid-latitude ionosonde chain during a series of storms in March 2012. Vertical dashed lines show SSC of the storms; the bottom panel displays Dst variations

phase on March 9 according to the ionosondes in Novosibirsk and Juliusruh and during the storm recovery phase on March 10 according to the ionosonde in Paratunka (Figure 5, a).

We have noted that, according to the data from all mid-latitude ionosondes over the territory of Eurasia, the negative ionospheric storm effect was manifested during the main and recovery phases of the S4 magnetic storm on March 15, 2012 (see Figure 4, b). A strong increase in the maximum ionization height h_mF2 for this moderate magnetic storm was detected by the ionosonde in Paratunka immediately after SSC and during the main phase on March 15; by the ionosonde in Novosibirsk, during the main phase on March 16 (Figure 5). While the minimum values of ionization were observed over Western Europe on March 16, 2012, according to the Juliusruh ionosonde data, the increase in the height of maximum ionization over this region was significantly smaller than over Siberia and the Far East. Of interest is the increase in h_mF2 according to the Yakutsk ionosonde data on March 18. The increase in h_mF2 is likely to be related to the CH HSS event that accompanied the magnetic storm during the recovery phase from March 16 to 18.

During the effects of positive ionospheric storms, the absolute deviation dh_mF2 decreased to $-40 \div -60$ km. The same values of dh_mF2 were observed under conditions when the ionosphere began to recover to ionization values under undisturbed conditions. For example, for the S4 magnetic storm on March 15, the ionospheric ionization began to recover on March 18 initially in the region of $\sim 80^\circ$ to 110° E (ionosondes in Novosibirsk

and Irkutsk) (see Figures 4, a; 5), where the level of GMF variations is always low compared to neighboring longitude regions (see Figure 3, a).

DISCUSSION OF THE RESULTS OF EXPERIMENTAL DATA ANALYSIS

Ionospheric effects of the long period of geomagnetic disturbances in March 2012 have been analyzed in a number of papers [Habarulema et al., 2015, 2016; Verkhoglyadova et al., 2016; Belehaki et al., 2017; Krypiak-Gregorczyk, 2019]. Belehaki et al. [2017] have studied the March 7–10, 2012 magnetic storm (S1, S2) by analyzing data from ionosondes and GPS receivers in Durba (Belgium) and Ebro (Spain), as well as simulation results. The positive ionospheric storm effect over Western Europe was observed on March 7, 2012. According to the authors, a significant increase in TEC at midlatitudes was caused by the effect of the equatorial super fountain associated with PPEFs in equatorial latitudes.

Habarulema et al. [2015, 2016] also detected the positive ionospheric storm effect over Africa during the March 8–10, 2012 magnetic storm (S1, S2) in both hemispheres. A cause of the positive ionospheric storm was the expansion of the equatorial ionization anomaly to midlatitudes. Nonetheless, Habarulema et al. [2015, 2016] noted that physics of this particular geomagnetic disturbance was complex. During the entire disturbed period on March 7–17, 2012, a series of S1–S4 geomagnetic storms took place [Tsurutani et al., 2014].

Therefore, after March 10, 2012 (S3–S4), the scenario for the ionospheric response to a geomagnetic disturbance changed. Some stations of the meridional chain of GPS receivers and ionosondes at hand recorded the negative ionospheric storm effect. This may be interpreted as dissipation of the superfountain energy when the structure of the equatorial anomaly expands to the pole. According to the authors, there is a superposition of the effect of increasing electron density due to the expansion of the equatorial ionization anomaly to the background ionosphere and the effect of changing the composition of the thermosphere of auroral origin, which is responsible for the development of the negative ionospheric storm effect. In such cases, there may be a switch between the ionospheric storm positive and negative phases. Global maps of TEC showed simultaneous propagation of large-scale traveling ionospheric disturbances over Africa both to the pole and to the equator during the same period of the geomagnetic storm.

Verkhoglyadova et al. [2016] have examined ionospheric effects of the March 15–18, 2012 magnetic storm S4. To analyze the effects in the ionosphere, they used global maps of vertical TEC distribution, which showed a weak temporal response to the magnetic storm in middle and low latitudes.

Krypiak-Gregorczyk [2019] presents results of a detailed study into variations in ionospheric parameters over Western Europe based on measurements of GPS/GLONASS receivers and ionosondes (Rome, Juliusruh) during magnetic storms S1–S4 on March 7, 9, 12, and 15, 2012. March 7 and 8, 2012 (S1) were characterized by positive changes in TEC. However, the level of these changes depended on latitude. The greatest increase in TEC occurred during S2 on March 9 in the southernmost latitude region and was associated with the superfountain effect in the equatorial ionosphere. With increasing latitude, TEC decreased. Moreover, at 50° N there was a clear transition from the effect of a positive ionospheric storm to a negative one. The negative ionospheric storm is observed at all longitudes and latitudes above 50° N under study. This different character of the ionospheric storm for different latitude regions on March 9, 2012 is associated with CME on March 7, which arrived in Earth two days later. The S3 event on March 12 caused a significant one-day increase in TEC. The last storm S4 on March 15 was preceded by an increase in TEC, followed by its decrease; as a result, the negative phase of the ionospheric storm was observed. The next day, March 16, saw the largest decrease in TEC for the entire period of interest.

The results of the analysis of ionospheric ionization variations during the series of magnetic storms in March 2012 based on measurements of mid-latitude Eurasian ionosondes we report in this paper confirm the conclusions made in [Habarulema et al., 2015, 2016; Verkhoglyadova et al., 2016; Belehaki et al., 2017; Krypiak-Gregorczyk, 2019]. Just like Habarulema et al. [2015, 2016], we emphasize the complex physics of this long magnetically disturbed period with transitions of the effects of positive and negative ionospheric storms.

Such transitions occurred during the S1 recovery phase when the positive effect of the ionospheric storm was replaced by the negative one over Paratunka and Yakutsk; during the S2 main and recovery phases, a short-term phase change of the ionospheric storm from positive to negative occurred twice over Irkutsk and Novosibirsk; during the S2 recovery phase, the negative effect of the ionospheric storm was replaced by the positive one over Moscow and Juliusruh.

The change in the effects of positive and negative ionospheric storms during the series of magnetic storms in March 2012 might have been associated with the joint action of competing processes affecting ionization in the mid-latitude region, whose sources are located in the auroral and equatorial ionosphere. The authors of [Habarulema et al., 2015, 2016; Belehaki et al., 2017] attribute the positive ionospheric storm effect to the superfountain effect in the equatorial latitudes during the period March 7–10, 2012.

Switching between the positive and negative phases of the ionospheric storm was also observed for the magnetic storm in March 2015 [Shpynev et al., 2018; Chernigovskaya et al., 2021a] and for the storm in October 2016 [Chernigovskaya et al., 2021b], which also developed under equinox conditions. The transition from one ionospheric storm phase to another is more typical of winter than of summer [Burešová et al., 2007]. The probability of the scenario with a change in the ionospheric storm effect also increases with a decrease in latitude. For storms at the equinox, this relationship is not clearly defined. However, March and October in the mid-latitude range of interest most likely belong to the winter half of the year.

Krypiak-Gregorczyk [2019] has noted that a negative ionospheric storm was observed at all the longitudes of Western Europe above 50° N under study for the March 7 and 9 magnetic storms. We also point out the negative ionospheric storm effect according to the data from the ionosondes in Moscow and Juliusruh during the S1 and S2 main phases. The conclusions about the positive ionospheric storm effect for the March 12 magnetic storm and the long-term negative ionospheric storm effect for the March 15 magnetic storm over the European region also coincide.

Earlier in [Shpynev et al., 2018; Chernigovskaya et al., 2019, 2020, 2021a, 2021b], the longitude inhomogeneity of the ionosphere over Eurasia has been revealed, one of the main causes of which was the GMF configuration. The irregular structure of the longitudinal variability of the GMF strength components is a consequence of spatial anomalies of various scales in the background geomagnetic field, as well as the mismatch between the magnetic and geographic poles. The zones of maximum GMF variations correspond to the zones of enhanced penetration of geomagnetic disturbances from high to middle latitudes. During magnetically disturbed periods, two zones of strong GMF variations are formed symmetrically about the meridian of the geomagnetic pole near longitudes of ~40° E and ~130° E. In these longitude regions, strong negative ionospheric disturbances occur, i.e. decreases in f_oF_2 , which is associated

with a decrease in the F2-layer maximum electron density. In the longitudinal sector 80° – 110° E (zone of the East Siberian Continental Magnetic Anomaly), the level of GMF variations is always low. In this regard, the ionosphere has a positive anomaly over Eurasia at longitudes $\sim 80^{\circ}$ – 110° and recovers earlier than other longitude regions after geomagnetic disturbances [Shpynev et al., 2018; Chernigovskaya et al., 2019, 2020, 2021a, 2021b].

Moro et al. [2019], using the results of a study into variations in ionospheric parameters according to data from two low-latitude ionosondes located at approximately the same latitudes in the Northern and Southern hemispheres, have found that during geomagnetic storms the variability of ionospheric parameters is higher for the ionosonde in Santa Maria (Brazil), located in the South American Magnetic Anomaly, than for the ionosonde in Wuhan (China). The authors attribute this feature of ionospheric effects on geomagnetic disturbances to the presence of regional features of the main GMF in South America.

Analysis of the response of the mid-latitude ionosphere over Eurasia to long-term geomagnetic disturbances in March 2012 also showed the manifestation of longitude inhomogeneity of ionospheric ionization associated with spatial anomalies in background GMF. In $\sim 80^{\circ}$ – 110° E, the ionosphere as a whole had an increased level of electron density at the height of the maximum ionospheric ionization (red contour in Figure 4, *a*). The F2-layer critical frequencies were as high as ~ 9 – 10 MHz according to ionosonde measurements in Novosibirsk and Irkutsk. For the S3 and S4 events, the ionosphere over Siberia began to recover to ionization values in undisturbed conditions earlier than other longitude regions in Eurasia (Figure 4, *b*). This longitudinal sector features a low level of GMF variations in the East Siberian Continental Magnetic Anomaly (Figure 3, *a*) [Shpynev et al., 2018; Chernigovskaya et al., 2021a]. In the regions adjacent to the longitudinal sector $\sim 80^{\circ}$ – 110° E (the Far East $\sim 120^{\circ}$ – 140° E, Western Siberia and Eastern Europe $\sim 40^{\circ}$ – 60° E), strong negative ionospheric disturbances are observed (blue contours in Figure 4, *a*). These regions correspond to zones of enhanced penetration of geomagnetic disturbances from high to middle latitudes, and they show increased GMF variations under disturbed geomagnetic conditions (Figure 3, *a*).

CONCLUSIONS

The study into variations in ionospheric parameters at midlatitudes of the Northern Hemisphere over Eurasia based on data from ionosondes and magnetometers of the global network INTERMAGNET during the series of geomagnetic storms in March 2012 confirms the conclusion made earlier in [Shpynev et al., 2018; Chernigovskaya et al., 2019, 2020, 2021a, 2021b] that the structure of the magnetosphere-ionosphere current system during magnetic storms depends on spatial anomalies of the main geomagnetic field, manifested in variations in the GMF and ionospheric parameters.

We have confirmed the nonuniform structure of the longitudinal variability of the GMF strength components due to the mismatch between geographic and geomagnetic poles (UT effect), as well as due to spatial anomalies of different scales in the main geomagnetic field.

The longitudinal features of the structure of the main GMF and its variations under changes in geomagnetic conditions lead to pronounced longitude inhomogeneity in the ionosphere.

During the storm main phase, the longitudinal dynamics of geomagnetic and ionospheric disturbances is almost synchronous at high and middle latitudes and is associated with the global movement of the magnetospheric convection zone from high to middle latitudes.

During a magnetic storm, variations in the main GMF become significant. They can play an important role in forming longitude inhomogeneities of the ionosphere, especially during the storm recovery phase.

We have pointed out the complex physics of the long magnetically disturbed period in March 2012 with switching between the ionospheric storm positive and negative phases during the same period of the magnetic storm for different spatial regions. The change in the ionospheric storm effects during the period under study might have been linked to the superposition in the mid-latitude region of competing processes affecting ionospheric ionization, whose sources are located in the auroral ionosphere (a series of intense solar activity events that generated geomagnetic storms on March 7, 9, 12, 15, 2012 and a significant disturbance of the high-latitude atmosphere and ionosphere), as well as in the equatorial ionosphere (the superfountain effect at equatorial latitudes on March 7–10, 2012).

During the storm recovery phase, the greatest drop in ionization was observed in the zones of strong GMF variations at longitudes $\sim 120^{\circ}$ – 140° E (according to the data from the Yakutsk and Paratunka ionosondes) and $\sim 40^{\circ}$ – 60° E (according to the data from the Moscow and Ekaterinburg ionosondes).

Over the Siberian region of Eurasia at longitudes $\sim 80^{\circ}$ – 110° E (according to data from Novosibirsk and Irkutsk ionosondes), the ionosphere as a whole had an increased level of ionization and began to recover earlier than other longitudinal zones after geomagnetic disturbances due to the low level of GMF variations at these longitudes.

The longitudinal features of variations in ionospheric parameters during the series of magnetic storms in March 2012, the strong storm in October 2016 [Chernigovskaya et al., 2021b] and the extreme storm in March 2015 [Shpynev et al., 2018; Chernigovskaya et al., 2021a] under equinox conditions with the identical background (undisturbed) ionosphere with a pronounced transition from daytime conditions to nighttime ones were similar to the analogous pronounced manifestation of longitude variations associated with the dependence on the variability of the main GMF variations.

The work was financially supported by the Ministry of Science and Higher Education of the Russian Federa-

tion (project FWZZ-2022-0019 for IPGG SB RAS). Experimental data was partially obtained using the equipment of Shared Equipment Center “Angara” (ISTP SB RAS) [<http://ckp-rf.ru/ckp/3056>].

REFERENCES

- Astafyeva E.I. Dayside ionospheric uplift during strong geomagnetic storms as detected by the CHAMP, SAC-C, TOPEX and Jason-1 satellites. *Adv. Space Res.* 2009, vol. 43, iss. 11, pp. 1749–1756. DOI: [10.1016/j.asr.2008.09.036](https://doi.org/10.1016/j.asr.2008.09.036).
- Astafyeva E., Zakharenkova I, Förster M. Ionospheric response to the 2015 St. Patrick’s Day storm: A global multi-instrumental overview. *J. Geophys. Res.: Space Phys.* 2015, vol. 120, pp. 9023–9037. DOI: [10.1002/2015JA021629](https://doi.org/10.1002/2015JA021629).
- Behlchaki A., Kutiev I., Marinov P., Tsagouri I, Koutroumbas K., Elias P. Ionospheric electron density perturbations during the 7–10 March 2012 geomagnetic storm period. *Adv. Space Res.* 2017, vol. 59, iss. 4, pp. 1041–1056. DOI: [10.1016/j.asr.2016.11.031](https://doi.org/10.1016/j.asr.2016.11.031).
- Blanc M., Richmond A.D. The ionospheric disturbance dynamo. *J. Geophys. Res.* 1980, vol. 85, pp. 1669–1686.
- Buonsanto M.J. Ionospheric storms — a review. *Space Sci. Rev.* 1999, vol. 88, pp. 563–601.
- Burešová D., Laštovička J., De Franceschi G. Manifestation of strong geomagnetic storms in the ionosphere above Europe. *Space Weather*. Springer, 2007, pp. 185–202.
- Chernigovskaya M.A., Shpynev B.G., Khabituev D.S., Ratovskii K.G., Belinskaya A.Yu., Stepanov A.E., et al. Dolgotnye variatsii ionosfernykh i geomagnitnykh parametrov v severnom polusharii vo vremya sil’nykh magnitnykh bur’ 2015 g. (Longitudinal variations of geomagnetic and ionospheric parameters during severe magnetic storms in 2015), *Sovremennye problemy distantsionnogo zondirovaniya Zemli iz kosmosa*, 2019, vol. 16, no. 5, pp. 336–347. DOI: [10.21046/2070-7401-2019-16-5-336-347](https://doi.org/10.21046/2070-7401-2019-16-5-336-347). (In Russian).
- Chernigovskaya M.A., Shpynev B.G., Yasyukevich A.S., Khabituev D.S. Ionosfernaya dolgotnaya izmenchivost’ v severnom polusharii vo vremya magnitnykh bur’ po dannym ionozondov i GPS/GLONASS (Ionospheric longitudinal variability in the Northern Hemisphere during magnetic storm from the ionosonde and GPS/GLONASS data), *Sovremennye problemy distantsionnogo zondirovaniya Zemli iz kosmosa*, 2020, vol. 17, no. 4, pp. 269–281. DOI: [10.21046/2070-7401-2020-17-4-269-281](https://doi.org/10.21046/2070-7401-2020-17-4-269-281). (In Russian).
- Chernigovskaya M.A., Shpynev B.G., Yasyukevich A.S., Khabituev D.S., Ratovskii K.G., Belinskaya A.Yu., et al. Longitudinal variations of geomagnetic and ionospheric parameters in the Northern Hemisphere during magnetic storms according to multi-instrument observations. *Adv. Space Res.* 2021a, vol. 67, no. 2, pp. 762–776. DOI: [10.1016/j.asr.2020.10.028](https://doi.org/10.1016/j.asr.2020.10.028).
- Chernigovskaya M.A., Shpynev B.G., Yasyukevich A.S., Khabituev D.S., Ratovskii K.G., Belinskaya A.Yu., et al. Longitudinal variations in the response of the mid-latitude ionosphere of the Northern Hemisphere to the October 2016 geomagnetic storm using multi-instrumental observations. *Current problems in Remote Sensing of the Earth From Space*. 2021b, vol. 18, no. 5, pp. 305–317. DOI: [10.21046/2070-7401-2021-18-5-305-317](https://doi.org/10.21046/2070-7401-2021-18-5-305-317). (In Russian).
- Danilov A.D. Ionospheric F-region response to geomagnetic disturbances. *Adv. Space Res.* 2013, vol. 52, pp. 343–366. DOI: [10.1016/j.asr.2013.04.019](https://doi.org/10.1016/j.asr.2013.04.019).
- Dmitriev A.V., Huang C.-M., Brahmanandam P.S., Chang L.C., Chen K.-T., Tsai L.-C. Longitudinal variations of positive dayside ionospheric storms related to recurrent geomagnetic storms. *J. Geophys. Res.: Space Phys.* 2013, vol. 118, pp. 6806–6822. DOI: [10.1002/jgra.50575](https://doi.org/10.1002/jgra.50575).
- Dudok de Wit T., Watermann J. Solar forcing of the terrestrial atmosphere. *Comptes Rendus Geoscience*. 2009, vol. 342, no. 4-5, pp. 259–272. DOI: [10.1016/j.crte.2009.06.001](https://doi.org/10.1016/j.crte.2009.06.001).
- Habarulema J.B., Katamzi Z.T., Yizengaw E. First observations of poleward large-scale traveling ionospheric disturbances over the African sector during geomagnetic storm conditions. *J. Geophys. Res.: Space Phys.* 2015, vol. 120, pp. 6914–6929. DOI: [10.1002/2015JA021066](https://doi.org/10.1002/2015JA021066).
- Habarulema J.B., Katamzi Z.T., Yizengaw E., Yamazaki Y., Seemala G. Simultaneous storm time equatorward and poleward large-scale TIDs on a global scale. *Geophys. Res. Lett.* 2016, vol. 43, pp. 6678–6686. DOI: [10.1002/2016GL069740](https://doi.org/10.1002/2016GL069740).
- Hafstad L.R., Tuve M.A. Note on Kennelly-Heaviside layer observations during a magnetic storm. *Terrestrial magnetism and atmospheric electricity*. 1929, vol. 34, no. 1, pp. 39–43.
- Krypiak-Gregorczyk A. Ionosphere response to three extreme events occurring near spring equinox in 2012, 2013 and 2015, observed by regional GNSS-TEC model. *J. Geodesy*. 2019, vol. 93, pp. 931–951. DOI: [10.1007/s00190-018-1216-1](https://doi.org/10.1007/s00190-018-1216-1).
- Kunitsyn V.E., Padokhin A.M., Kurbatov G.A., Yasyukevich Yu.V., Morozov Yu.V. Ionospheric TEC estimation with the signals of various geostationary navigational satellites. *GPS Solutions*. 2016, vol. 20, pp. 877–884. DOI: [10.1007/s10291-015-0500-2](https://doi.org/10.1007/s10291-015-0500-2).
- Li Q., Liu L., Balan N., Huang H., Zhang R., Chen Y., Le H. Longitudinal structure of the midlatitude ionosphere using COSMIC electron density profiles. *J. Geophys. Res.: Space Phys.* 2018, vol. 123, pp. 8766–8777. DOI: [10.1029/2017JA024927](https://doi.org/10.1029/2017JA024927).
- Loewe C.A., Prölss G.W. Classification and mean behavior of magnetic storms. *J. Geophys. Res.* 1997, vol. 102, iss. A7, pp. 14,209–14,213.
- Mansilla G.A. Mid-latitude ionospheric effects of a great geomagnetic storm. *J. Atmos. Solar-Terr. Phys.* 2004, vol. 66, pp. 1085–1091. DOI: [10.1016/j.jastp.2004.04.003](https://doi.org/10.1016/j.jastp.2004.04.003).
- Mansilla G.A., Zossi M.M. Longitudinal Variation of the Ionospheric Response to the 26 August 2018 Geomagnetic Storm at Equatorial/Low Latitudes. *Pure Appl. Geophys.* 2020, vol. 177, pp. 5833–5844. DOI: [10.1007/s00024-020-02601-1](https://doi.org/10.1007/s00024-020-02601-1).
- Matsushita S. A study of the morphology of ionospheric storms. *J. Geophys. Res.* 1959, vol. 64, no. 3, pp. 305–321. DOI: [10.1029/JZ064i003p00305](https://doi.org/10.1029/JZ064i003p00305).
- Mendillo M. Storms in the ionosphere: Patterns and processes for total electron content. *Rev. Geophys.* 2006, vol. 44, RG4001. DOI: [10.1029/2005RG000193](https://doi.org/10.1029/2005RG000193).
- Moro J., Xu J., Denardini C.M., Resende L.C.A., Silva R.P., Liu Z., Li H., Yan C., Wang C., Schuch N.J. On the sources of the ionospheric variability in the South American Magnetic Anomaly during solar minimum. *J. Geophys. Res.:Space Phys.* 2019, vol. 124, pp. 7638–7653. DOI: [10.1029/2019JA026780](https://doi.org/10.1029/2019JA026780).
- Polyakov V.M., Shchepkin L.A., Kazimirovsky E.S., Kokourov V.D. Ionosfernye processy (Ionospheric processes), Novosibirsk: Nauka Publ., 1968, 535 p. (In Russian).
- Prölss G.W. Ionospheric F-region storms. *Handbook of atmospheric electrodynamics*. CRC Press, Boca Raton. 1995, vol. 2, Ch. 8, pp. 195–248.
- Prölss G.W., Brace L.H., Mayr H.G., Carignan G.R., Killeen T.L., Klobuchar J.A. Ionospheric storm effects at subauroral latitudes: A case study. *J. Geophys. Res.* 1991, vol. 96, pp. 1275–1288.
- Ratovsky K.G., Klimenko M.V., Klimenko V.V., Chirik N.V., Korenkova N.A., Kotova D.S. After-effects of geomagnetic storms: statistical analysis and theoretical explanation. *Solar-Terr. Phys.* 2018, vol. 4, iss. 4, pp. 26–32. DOI: [10.12737/stp-44201804](https://doi.org/10.12737/stp-44201804). 32–42.
- Rishbeth H. How the thermospheric circulation affects the ionospheric F2-layer. *J. Atmos. Solar-Terr. Phys.* 1998, vol. 60, pp. 1385–1402.

Shpynev B.G., Zolotukhina N.A., Polekh N.M., Ratovsky K.G., Chernigovskaya M.A., Belinskaya A.Yu., et al. The ionosphere response to severe geomagnetic storm in March 2015 on the base of the data from Eurasian high-middle latitudes ionosonde chain. *J. Atmos. Solar-Terr. Phys.* 2018, vol. 180, pp. 93–105. DOI: [10.1016/j.jastp.2017.10.014](https://doi.org/10.1016/j.jastp.2017.10.014).

Tsurutani B., Mannucci A., Iijima B., Abdu M.A., Sobral J.H.A., Gonzalez W., et al. Global dayside ionospheric uplift and enhancement associated with interplanetary electric fields. *J. Geophys. Res.* 2004, vol. 109, A08302. DOI: [10.1029/2003JA010342](https://doi.org/10.1029/2003JA010342).

Tsurutani B., Echer E., Shibata K., Verkhoglyadova O., Mannucci A., Gonzalez W., et al. The interplanetary causes of geomagnetic activity during the 7–17 March 2012 interval: a CAWSES II overview. *J. Space Weather Space Climate.* 2014, vol. 4, no. A02. DOI: [10.1051/swsc/2013056](https://doi.org/10.1051/swsc/2013056).

Verkhoglyadova O.P., Tsurutani B.T., Mannucci A.J., Mlynczak M.G., Hunt L.A., Paxton L.J., Komjathy A. Solar wind driving of ionosphere-thermosphere responses in three storms near St. Patrick's Day in 2012, 2013, and 2015. *J. Geophys. Res.: Space Phys.* 2016, vol. 121, pp. 8900–8923. DOI: [10.1002/2016JA022883](https://doi.org/10.1002/2016JA022883).

Wang H., Zhang K. Longitudinal structure in electron density at mid-latitudes: upward-propagating tidal effects. *Earth, Planets and Space.* 2017, iss. 1, article id. 11. DOI: [10.1186/s40623-016-0596-9](https://doi.org/10.1186/s40623-016-0596-9).

URL: <http://www.intermagnet.org> (accessed July 19, 2022).

URL: <http://wdc.kugi.kyoto-u.ac.jp> (accessed July 19, 2022).

URL: <https://www.swpc.noaa.gov/noaa-scales-explanation> (accessed July 19, 2022).

URL: <http://ckp-rf.ru/ckp/3056> (accessed July 19, 2022).

Original Russian version: Chernigovskaya M.A., Shpynev B.G., Khabituev D.S., Ratovsky K.G., Belinskaya A.Yu., Stepanov A.E., Bychkov V.V., Grigorieva S.A., Panchenko V.A., Mielich J., published in *Solnechno-zemnaya fizika.* 2022. Vol. 8. Iss. 4. P. 46–56. DOI: [10.12737/szf-84202204](https://doi.org/10.12737/szf-84202204). © 2022 INFRA-M Academic Publishing House (Nauchno-Izdatelskii Tsentr INFRA-M)

How to cite this article

Chernigovskaya M.A., Shpynev B.G., Khabituev D.S., Ratovsky K.G., Belinskaya A.Yu., Stepanov A.E., Bychkov V.V., Grigorieva S.A., Panchenko V.A., Mielich J. Studying the response of the mid-latitude ionosphere of the Northern Hemisphere to magnetic storms in March 2012. *Solar-Terrestrial Physics.* 2022. Vol. 8. Iss. 4. P. 44–54. DOI: [10.12737/stp-84202204](https://doi.org/10.12737/stp-84202204).